The author greatly thanks Professor R. A. Cowley for valuable suggestions, discussions and assistance at all stages of this work. I also wish to thank T. W. Ryan for all technical and practical assistance, and R. J. Nelmes for practical advice.

This work was supported by the Science and Engineering Research Council and by the Royal Norwegian Council for Scientific and Industrial Research.

References

BLINC, R., BURGAR, M., SLAK, J., RUTAR, V. & MILIA, F. (1979). *Phys. Status Solidi A*, **56**, K65-K69.

COCHRAN, W. (1968). *Neutron Inelastic Scattering*, Vol. 1. Symp. Proc., Copenhagen, 1968. Vienna: International Atomic Energy Agency.

FAN, H.-F., YAO, J.-X., MAIN, P. & WOOLFSON, M. M. (1983). *Acta Cryst.* A**39**, 566-569.

FUKUI, M., ABE, R. & TSUCHIDA, K. (1983). *J. Phys. Soc. Jpn*, **52**, 4369-4376.

HASEBE, K., MASHIYAMA, H. & TANISAKI, S. (1980). *J. Phys. Soc. Jpn Lett.* **49**, 1633-1634.

HASEBE, K., MASHIYAMA, H. & TANISAKI, S. (1982). *J. Phys. Soc. Jpn Lett.* **51**, 2049-2050.

IIZUMI, M., AXE, J. D., SHIRANE, G. & SHIMAOKA, K. (1977). *Phys. Rev. B*, **15**, 4392-4411.

MASHIYAMA, H. (1980). *J. Phys. Soc. Jpn*, **49**, 2270-2277.

SAWADA, S., SHIROISHI, Y., YAMAMOTO, A., TAKASHIGE, M. & MATSUO, M. (1978). *Phys. Lett. A*, **67**, 56-58.

TSUCHIDA, K., IMAIZUMI, S., ABE, R. & SUZUKI, I. (1982). *J. Phys. Soc. Jpn*, **51**, 2199-2204.

WIESNER, J. R., SRIVASTAVA, R. C., KENNARD, C. H. L., DIVAIRA, M. & LINGAFELTER, E. C. (1967). *Acta Cryst.* **23**, 565-574.

WOLFF, P. M. DE (1974). *Acta Cryst.* A**30**, 777-785.

WOLFF, P. M. DE, JANSSEN, T. & JANNER, A. (1981). *Acta Cryst.* A**37**, 625-636.

YAMAMOTO, A. (1982). *Acta Cryst.* A**38**, 87-92.

Acta Cryst. (1985). B**41**, 336-341

The Location of Manganese and Calcium Ion Cofactors in Pea Lectin Crystals by Use of Anomalous Dispersion and Tuneable Synchrotron X-Radiation

BY H. EINSPAHR,* K. SUGUNA† AND F. L. SUDDATH‡

Department of Biochemistry, Institute of Dental Research and Comprehensive Cancer Center, University of Alabama at Birmingham, Birmingham, Alabama 35294, *USA*

AND G. ELLIS, J. R. HELLIWELL AND M. Z. PAPIZ

Department of Physics, University of Keele, Keele, Staffordshire ST5 5BG and SERC, Daresbury Laboratory, Daresbury, Warrington, Cheshire WA4 4AD, England

(*Received* 26 *July* 1984; *accepted* 17 *April* 1985)

Abstract

The location of the Mn^{2+} and Ca^{2+} sites in single crystals of pea lectin by enhancement of the anomalous dispersion of the Mn^{2+} ions with a wavelength near the Mn *K* absorption edge on the tuneable, focused X-ray spectrometer for protein crystallography at the Daresbury Synchrotron Radiation Source is reported. Anomalous difference Fourier maps [Kraut (1968). *J. Mol. Biol.* **35**, 511-512] calculated with film data at wavelengths of 1·860 and 1·488 Å and with diffractometer data at 1·5418 Å are compared with one another and with the native electron density map. Accurate identification and location of the Mn^{2+} and Ca^{2+} ions is possible, based on the large relative difference in *f''* anomalous components of the ions in the anomalous difference Fourier maps; such is not the case, based on the relative difference in atomic numbers of the ions, in the native electron density map.

Intense, tuneable synchrotron X-radiation is being increasingly used in data collection for protein crystal structure analysis. In particular, anomalous-dispersion effects at specific absorption edges of bound metal ions can be optimized or changed in a controlled way by finely varying the synchrotron X-ray wavelength. In the case of proteins with more than one kind of metal cofactor, differences in *f''* can be used to distinguish among anomalous-scattering cofactors of otherwise similar atomic number. In the present study the difference in the anomalous-dispersion coefficients of calcium ions (18 electrons) and

* Present address: The Upjohn Company, Physical and Analytical Chemistry, 7255-209-1 Kalamazoo, Michigan 49001, USA.

† Present address: Laboratory of Molecular Biology, National Institute of Arthritis, Diabetes & Kidney Diseases, NIH, Bethesda, Maryland 20205, USA.

‡ Present address: School of Chemistry, Georgia Institute of Technology, Atlanta, Georgia 30332, USA.

0108-7681/85/050336-06$01.50

Table 1. *Estimated anomalous-dispersion intensity differences at different wavelengths* [*equation* (1)]

(1) A value for f_0 of 7 e is assumed since this is approximately the mean atomic scattering factor for proteins comprising mainly C, N, O.
(2) The expected intensity difference as a result of temperature factors over the limited range ($\infty - 3{\cdot}0$ Å) is ignored.
(3) Values of f'' for Mn and Ca were calculated by a program originating from Cromer (1983, and references cited therein). The absence of any X-ray absorption near-edge structure is assumed in these calculations (see text).
(4) The overall values of f'' and $\langle|\Delta I_{anom}|\rangle/\langle I\rangle$ (added in quadrature) are those given in the column labeled 'Mn + Ca'. These are the values that should be compared to those in Table 2.
(5) $\langle|\Delta I_{anom}|\rangle/\langle I\rangle$ here and in equation (2) is derived from the work of Crick & Magdoff (1956).

		Mn $\langle\|\Delta I_{anom}\|\rangle/\langle I\rangle$			Ca $\langle\|\Delta I_{anom}\|\rangle/\langle I\rangle$			Mn + Ca $\langle\|\Delta I_{anom}\|\rangle/\langle I\rangle$
λ(Å)	f''_{Mn} (electrons)	1 atom (%)	2 atoms (%)	f''_{Ca} (electrons)	1 atom (%)	2 atoms (%)	f''_{Mn+Ca} (electrons)	4 atoms (%)
1·488	2·651	1·81	2·56	1·209	0·83	1·17	2·91	2·81
1·5418	2·809	1·92	2·71	1·287	0·88	1·24	3·09	2·98
1·860	3·816	2·61	3·69	1·779	1·22	1·72	4·21	4·07

manganese ions (23 electrons) has been exploited in this way. Synchrotron radiation (SR) from the Daresbury Synchrotron Radiation Source (SRS) has been used to enhance the imaginary coefficient f'' by tuning the wavelength close to the Mn K edge at 1·896 Å. This paper describes some technical details of the data collection on the SRS and compares the anomalous difference Fourier maps (Kraut, 1968) and the native protein electron density map. It will be seen that the use of SR resolved ambiguities in both identity and position of the metal ions in pea lectin.

Background

Details of the pea lectin structure analysis

Pea lectin crystallizes in space group $P2_12_12_1$ with cell dimensions $a = 50{\cdot}73$ (2), $b = 61{\cdot}16$ (2), and $c = 136{\cdot}59$ (8) Å. The estimated mass of protein per asymmetric unit is 49 000 daltons (two monomers) with 44% of the crystal being solvent by volume. Each monomer binds one Mn^{2+} ion and one Ca^{2+} ion. The crystal structure of pea lectin is being analyzed in Alabama and details have been presented at 6 Å (Meehan, McDuffie, Einspahr, Bugg & Suddath, 1982) and at 3 Å resolution (Einspahr, Suguna, Bugg & Suddath, 1983). The structure of the pea lectin molecule, a dimer, appears to resemble closely that of a dimer of the jack bean lectin, concanavalin A (Edelman, Cunningham, Reeke, Becker, Waxdal & Wang, 1972; Hardman & Ainsworth, 1972).

The 3 Å phase set used in the analyses described in this paper is essentially a composite phase set based on single-isomorphous-replacement and anomalous-scattering indications from overlapping data from eight crystals of a multi-site uranyl nitrate derivative collected with Cu $K\alpha$ X-radiation on an automated diffractometer. Variations in soak conditions, however, produced variations in patterns of uranyl site occupancies in the eight crystals, so that, in overlap regions, phase indications from crystals with different minor-site compositions are available. In addition, a 6 Å phase set from a *p*-chloromercuribenzene sulfonate derivative was used. The overall figure of merit for the phase set to 3 Å resolution is 0·69.

Determination of the metal-ion binding sites by use of anomalous-dispersion effects

Determining the binding sites of the metal ions in pea lectin involves distinguishing a total of two Mn^{2+} ions and two Ca^{2+} ions against a protein background of 49 000 daltons. If the Mn^{2+} ions could be dissociated from the native protein crystal, the intensity changes expected (approximately 10%) would be well within the range feasible for the application of isomorphous difference Fourier techniques to locate the Mn^{2+} sites. However, by selecting a wavelength near the absorption edge of Mn, it is possible to enhance the dispersion coefficients, f' and f'', of Mn and to locate the Mn^{2+} sites without resort to dissociation of the ions from the protein crystal.

The dispersion coefficients, f' and f'', take account of the variation of atomic scattering power with wavelength by providing an amplitude and phase correction to the normal scattering factor f_0 for an atom which has, therefore, an overall scattering factor of the form

$$f = f_0 + f'(\lambda) + if''(\lambda). \quad (1)$$

In the present study the imaginary coefficient f'', as a function of wavelength, has been utilized; Table 1 gives values of f'' for Mn and Ca at the wavelengths relevant to this paper. The expected average intensity change due to f''_{Mn} can be derived from the work of Crick & Magdoff (1956) as

$$(\langle|\Delta I_{anom}|\rangle/\langle I\rangle)_{Mn} = (2N_{Mn}/N)^{1/2}(2f''_{Mn}/f_0), \quad (2)$$

where $\Delta I_{anom} = I(hkl) - I(\bar{h}\bar{k}\bar{l})$. Table 1 gives the percentage changes, calculated with equation (2), expected for one or two Mn^{2+} ions based on f'' values at different wavelengths. At a wavelength of 1·860 Å, the predicted mean relative anomalous intensity difference is 2·61% for one Mn^{2+} ion and 3·69% for two Mn^{2+} ions. The successful location of the Mn^{2+}

ions in an anomalous difference Fourier map depends on the quality of the signal-to-noise ratio of the intensity measurements; the change of λ from 1·5418 Å, which is routinely used in the home laboratory, to 1·860 Å with synchrotron radiation (SR) enhances the f'' signals of Mn^{2+} and Ca^{2+} ions by 40%.

Experimental

Three native data sets have been collected. The first comprises the original diffractometer data obtained from one crystal on a conventional source at Cu $K\alpha$ wavelength and used in the 3 Å structural study. Absorption corrections were made on these intensity measurements by the φ-scan method of North, Phillips & Mathews (1968). The full experimental details of the diffractometer data collection have been described elsewhere (Meehan *et al.*, 1982; Einspahr *et al.*, 1983).

Two synchrotron data sets were collected. One, at a wavelength of 1·488 Å, is a high-resolution native protein data set that was collected to extend the pea lectin study beyond the 3 Å limit of the diffractometer data set. The other, at a wavelength of 1·860 Å, was collected to obtain anomalous-dispersion data with an enhanced manganese contribution. The 1·860 Å wavelength was a compromise chosen to accommodate an imprecisely known absorption-edge position (at approximately 1·896 Å) and to avoid unknown X-ray absorption near-edge structure (XANES). The wavelength used is therefore about 120 eV (1 eV = $1{\cdot}60\times10^{-19}$ J) away from the tabulated edge position. The 1·488 Å wavelength used for the reference data set was calibrated by scanning the absorption edge of a pure nickel foil. For the 1·860 Å wavelength, a pure manganese foil was used, and then the bent Ge(111) crystal monochromator was rotated a further 0·33° to be safely on the short λ side of the Mn edge [see Helliwell, Greenhough, Carr, Rule, Moore, Thompson & Worgan (1982) for a full explanation of the operational characteristics of the instrument]. The two data sets were collected on the oscillation camera with flat cassettes and a crystal-to-film distance of 55 mm, corresponding to resolution limits of 1·8 Å (for $\lambda = 1{\cdot}488$ Å) and 2·4 Å (for $\lambda = 1{\cdot}860$ Å). Fig. 1 shows an oscillation photograph recorded at 1·860 Å wavelength. Each data set used a crystal rotated about **b** through the 90° between **a*** and **c***; the blind region was not collected at 1·860 Å wavelength. During these data collections, the SRS operated at 2 GeV with mean circulating currents of 120 mA. Crystals were accurately aligned in order to maximize the sampling of Friedel pairs on the same film pack, thereby minimizing the effect of scaling errrors on the final measured anomalous differences. The films (CEA Reflex 25) were scanned on a Scandig drum scanner and processed with the latest version of A. J. Wonacott's oscillation film processing programs modified to take account of the synchrotron X-radiation beam geometry (Greenhough & Helliwell, 1982); since the Guinier setting of the instrument was used, account had to be taken only of the asymmetric cross-fire angles of the beam.

The anomalous difference Fourier syntheses followed that described by Kraut (1968) and are of the following form:

$$\mathrm{Im}\,[\Delta\rho(x)] = \frac{1}{V}\sum_{\mathbf{h}}[F(\mathbf{h}) - F(\bar{\mathbf{h}})]\sin[\alpha(\mathbf{h}) - 2\pi(\mathbf{h}\,.\,\mathbf{x})], \quad (3)$$

where the difference in the structure factor amplitudes is due primarily, in this case, to the Mn^{2+} and Ca^{2+} ions, and where $\alpha(\mathbf{h})$ is the phase of the protein structure factor derived from isomorphous replacement for each reflection **h**.

The different data sets contain different numbers of independent reflections. This is particularly true for the 1·860 Å data set, for which the blind region was not collected. For objective comparisons of the anomalous difference Fourier maps produced by the three native data sets, subsets were constructed that contained only acentric terms for which measured anomalous-scattering differences were available in all three sets. As absorption corrections were not made for the two SR data sets, these sets were scaled to the diffractometer set, which had been corrected for absorption, by use of a three-dimensional local scaling procedure. The synthesis excluded data for which

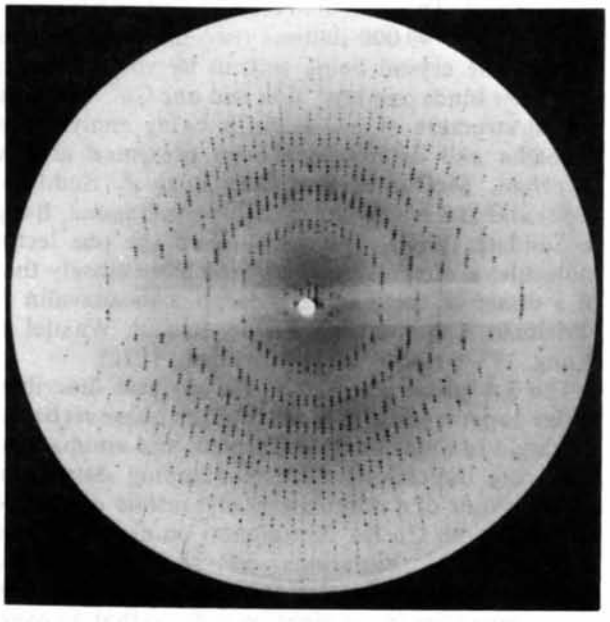

Fig. 1. Oscillation photograph recorded at the SRS from a single crystal of pea lectin at $\lambda = 1{\cdot}860$ Å. SRS operation was at 2 GeV with mean circulating current of 120 mA. Rotation range 2·5°, exposure time 250 s, resolution limit 2·4 Å.

Table 2. *Measured anomalous differences at different wavelengths*

(1) Merging R values [$R_{sym} = \sum_i (\sum_j |I_j - \bar{I}| / \sum_j I)$], where i indicates the sum over all reflections for which there is more than one measurement and j indicates the sum over averaged equivalents, are for the full data sets. The three subsets of data indicated by asterisks correspond to those composed only of reflections with measured anomalous-scattering differences in all three sets.
(2) The lower line in the entry for each data set or subset tabulates values for that fraction of the data with $|\Delta I_{anom}| < 4$ times the root-mean-square of ΔI_{anom} and $|\Delta I_{anom}| > \sigma(\Delta I_{anom})$.
(3) The discrepancy between calculated and observed values of $\langle|\Delta I_{anom}|\rangle/\langle I\rangle$ in Tables 1 and 2, respectively, can be largely attributed to errors in the measured intensities.

λ (Å)	$\langle\|\Delta I_{anom}\|\rangle/\langle I\rangle$ (%)	No. of data	Reflections with $\|\Delta I_{anom}\| > n\sigma$: $n=1$ (%)	$n=2$ (%)	$n=3$ (%)	R_{sym} (%)
1·860	10·7	5331	49·9	21·4	10·0	5·0
	16·4	2613				
1·488	9·3	6806	44·4	16·5	6·7	5·5
	15·6	2964				
1·5418	6·7	7305	43·2	13·2	3·5	5·8
	9·9	3113				
1·860*	10·5	5051	49·8	21·4	9·9	
	16·2	2470				
1·488*	8·5	5051	43·5	15·6	6·2	
	14·8	2144				
1·5418*	7·2	5051	43·8	13·5	3·6	
	10·6	2187				

$|\Delta F_{anom}|$ was greater than 4·0 times the root-mean-square of ΔF_{anom} or for which $|\Delta F_{anom}|$ was less than the estimated standard deviation of ΔF_{anom}, where $\Delta F_{anom} = F(hkl) - F(\bar{h}\bar{k}\bar{l})$. Of some 5000 terms common to the three subsets, the first exclusion condition generally eliminated between 25 and 30 terms, the latter between 2500 and 3000 terms. The rejection criteria are similar to those used by other workers for anomalous differences measured at Cu $K\alpha$ wavelength [see, for example, Hendrickson & Teeter (1981)].

Results and discussion

Table 2 shows anomalous difference statistics for data sets and subsets used in these analyses. Table 3 shows peak heights at metal-ion positions and other particulars of the anomalous difference Fourier maps calculated in these analyses. Three values are provided in Table 3 as means of assessing levels of noise in the three difference electron density maps. The first is the height of the highest uninterpreted peak in each map; the second is the absolute value of the height of the largest negative peak in each map; the third is the root-mean-square density value for each map. Figs. 2(*a*), 2(*b*) and 2(*c*), show sections through the Mn^{2+} and Ca^{2+} positions in each of the subset maps. As shown in Table 3, in two of the subset maps, the two highest peaks correspond to the two Mn^{2+} positions. These maps are those prepared from the 1·860

Table 3. *Peak heights, in arbitrary units, in anomalous difference Fourier syntheses*

(1) The three columns indicated by asterisks refer to maps calculated wth amplitudes from the three data subsets composed only of reflections with measured anomalous-scattering differences in all three sets.
(2) HUP = highest uninterpreted peak in each map; LNP = absolute value of the largest negative peak in each map; RMS = the root-mean-square electron density in each map.

	Data set (wavelength, Å) 1·860*	1·488*	1·5418*	1·5418
Mn(*A*)	307	180	193	289
Mn(*B*)	277	133	253	361
Ca(*A*)	137	100	111	172
Ca(*B*)	119	110	116	214
HUP	179	143	161	178
LNP	175	174	134	168
RMS	42	36	35	41

and 1·5418 Å data sets, and, while both maps are effective in pinpointing the Mn^{2+} positions, overall, the 1·860 Å map is the better. A comparison of the two SR maps, however, also shows that Mn^{2+} ion peaks in the 1·860 Å map are enhanced over those in the 1·488 Å map by factors ranging from 40 to 100% depending on how noise levels in the maps are assessed. Clearly, use of radiation near the Mn K absorption edge to collect intensity data has significantly enhanced the signal due to the Mn^{2+} ions, thereby assisting both the location and the identification of these ions in the structure. In none of the three subset maps were Ca^{2+} ion positions found to be above background levels; in retrospect, however, each map showed peaks at both Ca^{2+} ion positions.

Interestingly, when the full 1·5418 Å diffractometer set is used to prepare an anomalous difference Fourier map under the same $|\Delta F_{anom}|$ cut-off conditions as were used in the previous three maps, an improved map results in which four of the five largest peaks are at the positions of the four Mn^{2+} and Ca^{2+} ions (see Table 3 and Fig. 2*d*). This suggests that optimum results from anomalous-scattering differences are obtained when the full data set, within resolution limits, is employed and blind regions in the data are avoided.

Fig. 2(*e*) shows sections of the native protein electron density maps taken through the metal-ion sites as determined by the anomalous difference Fourier maps. At site *A* in this map, the peak heights of the Ca^{2+} and Mn^{2+} ions are reversed in contradiction to the anomalous difference Fourier maps. At site *B*, the Ca^{2+} ion position is shifted significantly in z compared with the anomalous maps.

The anomalous difference Fourier maps have allowed the unambiguous determination of the positions of the Mn^{2+} ions in the pea lectin crystal structure. In addition, the presence in each of the maps of an associated satellite peak near the Mn^{2+} ion peak in each monomer indicates the Ca^{2+} ion positions.

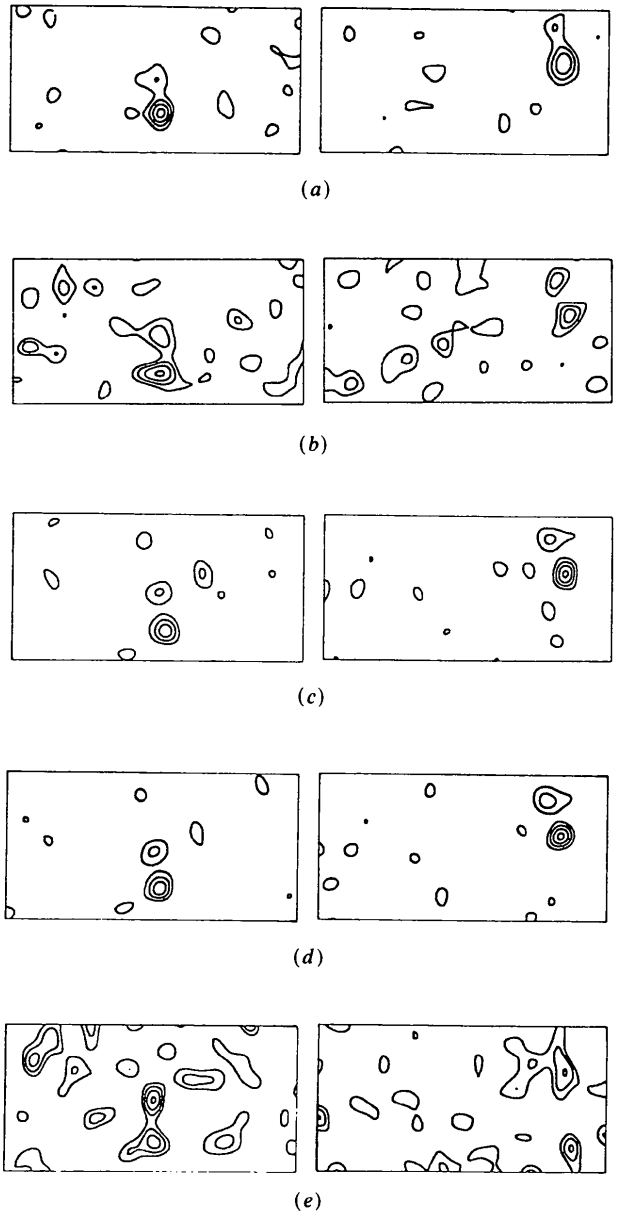

Fig. 2. General-plane sections through pairs of Mn^{2+} and Ca^{2+} ion positions in the anomalous difference Fourier maps and, in (*e*), the 3 Å native electron density map of pea lectin. Contours are in equal intervals of positive density and are chosen to show the highest peak in each map with four contour levels. Peaks corresponding to Ca^{2+} positions are satellites above and adjacent to Mn^{2+} peaks in each section and are two contour levels in height. Sections are through Mn(*A*) and Ca(*A*) (left-hand side) and Mn(*B*) and Ca(*B*) (right-hand side), respectively, (*a*) in the optimum 1·860 Å SR map (contour levels are multiples of 69), (*b*) for the analogous 1·488 Å SR map (contour levels at multiples of 43), (*c*) for the analogous 1·5418 Å map (contour levels at multiples of 60), (*d*) for the map based on the full 1·5418 Å data set (contour levels at multiples of 85), and (*e*) for the native electron density map (contour levels at multiples of 90). Maps span 0 to 1/4 in *z* along the horizontal direction and 17 Å perpendicular to *z* in the vertical direction. Normals of the general-plane sections relative to the crystallographic axes are for *A*, (−0·628, 0·778, 0) and, for *B*, (0·885, 0·465, 0).

The positions in fractional coordinates (*x*, *y*, *z*) are for monomer *A*, Mn(*A*) = (0·39, 0·64, 0·37) and Ca(*A*) = (0·32, 0·67, 0·37), and for monomer *B*, Mn(*B*) = (0·66, 0·40, 0·79) and Ca(*B*) = (0·71, 0·46, 0·80), with uncertainities of about 0·01. The distances between Ca^{2+} and Mn^{2+} ions in each monomer are 4·0 Å for site *A* and 4·7 Å for site *B*. The average of 4·3 Å agrees with the distance between the ions found in concanavalin A (Hardman, Agarwal & Freiser, 1982).

The anomalous difference Fourier maps derived from the SRS data, measured at two wavelengths, showed the specific enhancement of *f*″ at the metal ion sites. Moreover, the interpretation of all the anomalous maps agreed. Without the SRS data, the 1·5418 Å anomalous difference Fourier map would have been one piece of evidence in disagreement with the native electron density map. A number of other groups have used the anomalous-scattering effect, determined by measurements at more than one wavelength, to locate metal atoms and to determine phases of reflections (*e.g.* Hoppe & Jakubowski, 1975; Phillips, Wlodawer, Goodfellow, Watenpaugh, Sieker, Jensen & Hodgson, 1977; Adman, Stenkamp, Sieker & Jensen, 1978; Cascarano, Giacovazzo, Peerdeman & Kroon, 1982). The use of two wavelengths as described to locate and discriminate between two anomalous scatterers of similar atomic number based on Bijvoet differences is the first to be reported. The use of more than one wavelength to vary *f*′ and *f*″ may be expected to find increasing use in protein crystallography in the future.

The SERC and the University of Keele are thanked for support. We are grateful to D. T. Cromer for supplying us with the computer program for calculating the dispersion coefficients for any element at any wavelength. This work was supported in part by National Institutes of Health Grants DE-02670, CA-13148, GM-30551, and by a UAB Faculty Research Grant. HE is the recipient of NIH Research Career Development Award DE-00106.

References

ADMAN, E. T., STENKAMP, R. E., SIEKER, L. C. & JENSEN, L. H. (1978). *J. Mol. Biol.* **123**, 35-47.

CASCARANO, G., GIACOVAZZO, C., PEERDEMAN, A. F. & KROON, J. (1982). *Acta Cryst.* A**38**, 710-717.

CRICK, F. H. C. & MAGDOFF, B. S. (1956). *Acta Cryst.* **9**, 901-908.

CROMER, D. T. (1983). *J. Appl. Cryst.* **16**, 437.

EDELMAN, G. M., CUNNINGHAM, B. A., REEKE, G. N. JR, BECKER, J. W., WAXDAL, M. J. & WANG, J. L. (1972). *Proc. Natl Acad. Sci. USA*, **69**, 2580-2584.

EINSPAHR, H., SUGUNA, K., BUGG, C. E. & SUDDATH, F. L. (1983). *Program and Abstracts.* Am. Crystallogr. Assoc. Summer Meet., August 1-5, Snowmass, Colorado. Abstract PD15.

GREENHOUGH, T. J. & HELLIWELL, J. R. (1982). *J. Appl. Cryst.* **15**, 493-508.

HARDMAN, K. D., AGARWAL, R. C. & FREISER, M. J. (1982). *J. Mol. Biol.* **157**, 69-86.

HARDMAN, K. D. & AINSWORTH, C. F. (1972). *Biochemistry*, **11**, 4910-4919.
HELLIWELL, J. R., GREENHOUGH, T. J., CARR, P. D., RULE, S. A., MOORE, P. R., THOMPSON, A. W. & WORGAN, J. S. (1982). *J. Phys. E*, **15**, 1363-1372.
HENDRICKSON, W. A. & TEETER, M. M. (1981). *Nature (London)*, **290**, 107-113.
HOPPE, W. & JAKUBOWSKI, U. (1975). *Anomalous Scattering*, edited by S. RAMASESHAN & S. C. ABRAHAMS, pp. 437-461. Copenhagen: Munksgaard.
KRAUT, J. (1968). *J. Mol. Biol.* **35**, 511-512.
MEEHAN, E. J. JR, MCDUFFIE, J., EINSPAHR, H., BUGG, C. E. & SUDDATH, F. L. (1982). *J. Biol. Chem.* **257**, 13278-13282.
NORTH, A. C. T., PHILLIPS, D. C. & MATHEWS, F. S. (1968). *Acta Cryst.* A**24**, 351-359.
PHILLIPS, J. C. & HODGSON, K. O. (1980). *Acta Cryst.* A**36**, 856-864.
PHILLIPS, J. C., WLODAWER, A., GOODFELLOW, J. M., WATENPAUGH, K. D., SIEKER, L. C., JENSEN, L. H. & HODGSON, K. O. (1977). *Acta Cryst.* A**33**, 445-455.

Acta Cryst. (1985). B**41**, 341-348

Location of 'Tailor-Made' Additives in the Crystal and their Effect on Crystal Habit. A Study on the Host-Additive System L-Asparagine-L-aspartic Acid Monohydrate

BY J. L. WANG, Z. BERKOVITCH-YELLIN AND L. LEISEROWITZ

Department of Structural Chemistry, The Weizmann Institute of Science, Rehovot 76100, *Israel*

(*Received* 23 *August* 1984; *accepted* 1 *April* 1985)

Abstract

The crystal structures of L-asparagine monohydrate and of the solid solution (0·85:0·15) L-asparagine–L-aspartic acid monohydrate were refined using low-temperature (103 K) X-ray diffraction data. The atomic positions of the overlapping (asparagine) $CONH_2$ and (aspartic acid) CO_2H groups were resolved by the refinement procedure. The aspartic acid adopts the (commonly observed) synplanar O=C–O–H conformation (1) rather than the alternative antiplanar conformation (2).

Introduction

This work is part of a systematic study on the effect of 'tailor-made' additives, present in solution during crystallization (Addadi, Berkovitch-Yellin, Weissbuch, Lahav & Leiserowitz, 1983). The term 'tailor-made' signifies a molecule very similar in structure to that of the host. It was found that such additives have a dramatic effect on crystal growth and habit. The effect was explained in terms of a two-step mechanism: preferential adsorption of the additive on specific crystal faces for which the modified part of the additive points away from the crystal interior. Once bound the additive perturbs the regular deposition of oncoming layers so lowering the rates of growth in these directions, generally accompanied by a concomitant increase in the surface area of these faces. Using appropriate additives it became possible to induce preselected changes in crystal morphology.

In all the host-additive systems that we have studied to date the crystallographic site and molecular conformation of the adsorbed additive were inferred from a variety of experimental and theoretical results (Addadi, Berkovitch-Yellin, Domb, Gati, Lahav & Leiserowitz, 1982; Berkovitch-Yellin, van Mil, Addadi, Idelson, Lahav & Leiserowitz, 1985; Berkovitch-Yellin, 1985) but not from diffraction methods. Thus we searched for a system where we could unambiguously map the atomic positions of the additive from diffraction data better to ascertain the intermolecular interactions involved in effecting the change in crystal morphology. The main difficulty in such an experiment arises from the generally low (<1%) amount of the occluded additive. A system suitable for such an analysis is that in which the additive would induce a significant change in habit through repulsive interactions, and yet be occluded in amounts convincingly detectable by diffraction, *e.g.* from 5% upwards. These two requirements are not quite compatible. Nevertheless we had found that aspartic acid could be occluded in amounts up to 20% inside the crystal of asparagine H_2O with a dramatic change in morphology (Addadi *et al.*, 1982). To generalize this finding, namely the pronounced effect of carboxylic acid additives on amide crystals, we studied a wide variety of host-additive systems $R CONH_2/R CO_2H$. We found that the carboxylic acid additives induce dramatic changes in the crystal habit of the corresponding host amide (Berkovitch-Yellin, Addadi, Idelson, Lahav & Leiserowitz, 1982). However, because the carboxyl O atom is a much

0108-7681/85/050341-08$01.50